

Spectral Efficiency for MIMO UWB Channel in Rectangular Metal Cavity

Zhen Hu, Robert Qiu, Dalwinder Singh

Department of Electrical and Computer Engineering, Center for Manufacturing Research, Tennessee Tech University, Cookeville TN, USA

Email: {zhu21, rqiu, dsingh21}@tntech.edu

Abstract—Wireless communication in confined metal environment such as rectangular metal cavity has attracted more and more attentions recently. The channel characteristics in such an environment are different from those in the traditional wireless communication environments: extremely rich multipath components make communication very challenging. Multiple input multiple output (MIMO) plus ultra-wideband (UWB) technique is promising for wireless communication in confined metal environment, since it can fully employ radio resources not only in space domain but also in frequency domain. This paper considers the fundamental limit about MIMO UWB channel in rectangular metal cavity when different spectrum-shaping schemes such as water filling, constant power water filling, time reversal, channel inverse, constant power spectrum density and minimum mean square error are employed at the transmitter. Meanwhile, the measured channel transfer function is used in this paper for analysis.

Index Terms—Spectral efficiency, MIMO, UWB, rectangular metal cavity, water filling, constant power water filling, time reversal, channel inverse, constant power spectrum density, minimum mean square error, power allocation

I. INTRODUCTION

Wireless communication in confined metal environment has attracted more and more attentions recently [1] because of the increasing demand of communication in confined metal environment such as intra-ship, intra-vehicle [2], intra-engine, manufacturing plant, assembly line, nuclear plant and so on. The channel characteristics in such an environment are different from those in the traditional wireless communication environments [3]: extremely rich multipath components make communication in confined metal environment very challenging.

Multiple input multiple output (MIMO) is an important breakthrough in the scientific research on wireless communication, by greatly increasing the spectral efficiency [4]. Ultra-wideband (UWB) technique can resolve the resonance caused by metal wall into many time-resolvable pulses. Time-varying fading is the hallmark of narrowband wireless communication. It seems safe to say that almost all the major progress made in wireless industry, such as MIMO and orthogonal frequency-division multiplexing (OFDM), has been motivated to exploit

fading through diversity. Fading caused by multipath, however, may be negligible for UWB communication using a sufficiently larger signal bandwidth [6]. So the UWB channel considered in this paper can be treated as deterministic channel. The dominant mechanism is the extremely dense multipath [3] [5].

This paper considers MIMO UWB channel for the fundamental limit using measured channel transfer function. The work in this paper is the extension of [3] [5]. We calculate spectral efficiencies when different spectrum-shaping schemes are employed. These spectrum-shaping schemes include water filling, time reversal, channel inverse and constant power spectrum density (PSD) [5]. Meanwhile, constant power water filling [7] and minimum mean square error (MMSE) are also considered in this paper for comparison. In [5], the power allocation among entries in the transmitted signal vector is not studied for time reversal. When power allocation is considered, the calculation for spectral efficiency of time reversal is converted into the optimization problem. How to solve the optimization problem is the critical issue in this paper. Deterministic algorithm and random algorithm are used here to solve the corresponding optimization problems respectively in order to get the optimal spectral efficiency in time reversal. The results of optimization problem can give us more intuitions to design the high performance system for wireless communication and deploy wireless sensor network (WSN) in confined metal environment.

The rest of the paper is organized as follows. Section 2 derives the formulas to calculate the spectral efficiencies when different spectrum-shaping schemes are used. Section 3 studies the spectral efficiency of time reversal with power allocation. In this section, the power allocation among different entries in the transmitted signal vector is considered. Section 4 describes the setup and procedure of channel sounding using Vector Network Analyzer (VNA) in frequency domain to obtain channel transfer function. Numerical results are presented in Section 5 and the conclusions are drawn in Section 6.

II. SPECTRAL EFFICIENCY CALCULATION

It is assumed that there are N_t transmitter antennas and N_r receiver antennas in the system. The diagram of MIMO UWB system is shown in Fig. 1.

The channel transfer function is $\mathbf{H}(f)$ with bandwidth $W = f_1 - f_0$ where $f_0 (> 0)$ is the starting frequency and

This paper is based on "MIMO capacity for UWB Channel in Rectangular Metal Cavity," by Z. Hu, D. Singh, and R. Qiu, which appeared in the Proceedings of SOUTHEASTCON 2008, Huntsville AL, USA, April 2008. © 2008 IEEE.

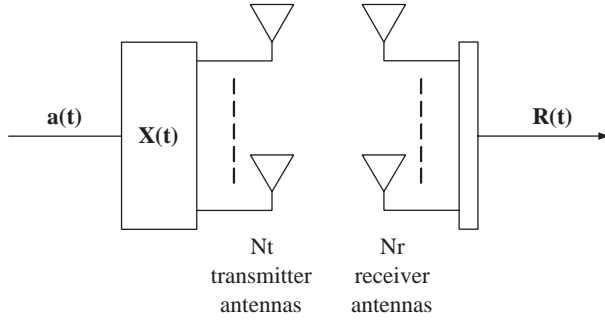


Figure 1. The diagram of MIMO UWB system.

$f_1 (> 0)$ is the end frequency.

$$\mathbf{H}(f) = \begin{bmatrix} H_{11}(f) & H_{12}(f) & \dots & H_{1N_t}(f) \\ H_{21}(f) & H_{22}(f) & \dots & H_{2N_t}(f) \\ \vdots & \vdots & \vdots & \vdots \\ H_{N_r,1}(f) & H_{N_r,2}(f) & \dots & H_{N_r,N_t}(f) \end{bmatrix} \quad (1)$$

where $\mathbf{H}_{mn}(f)$ is channel transfer function from the transmitter antenna n to the receiver antenna m . Its corresponding channel impulse response is

$$\mathbf{H}(t) = \begin{bmatrix} H_{11}(t) & H_{12}(t) & \dots & H_{1N_t}(t) \\ H_{21}(t) & H_{22}(t) & \dots & H_{2N_t}(t) \\ \vdots & \vdots & \vdots & \vdots \\ H_{N_r,1}(t) & H_{N_r,2}(t) & \dots & H_{N_r,N_t}(t) \end{bmatrix} \quad (2)$$

The spectrum-shaping filter at the transmitter side is

$$\mathbf{X}(t) = \begin{bmatrix} X_{11}(t) & X_{12}(t) & \dots & X_{1N_s}(t) \\ X_{21}(t) & X_{22}(t) & \dots & X_{2N_s}(t) \\ \vdots & \vdots & \vdots & \vdots \\ X_{N_t,1}(t) & X_{N_t,2}(t) & \dots & X_{N_t,N_s}(t) \end{bmatrix} \quad (3)$$

and its corresponding transfer function is

$$\mathbf{X}(f) = \begin{bmatrix} X_{11}(f) & X_{12}(f) & \dots & X_{1N_s}(f) \\ X_{21}(f) & X_{22}(f) & \dots & X_{2N_s}(f) \\ \vdots & \vdots & \vdots & \vdots \\ X_{N_t,1}(f) & X_{N_t,2}(f) & \dots & X_{N_t,N_s}(f) \end{bmatrix} \quad (4)$$

The input of the spectrum-shaping filter is the transmitted signal vector $\mathbf{a}(t)$. The entries of $\mathbf{a}(t)$ are $a_1(t)$, $a_2(t)$, ..., and $a_{N_s}(t)$,

$$\mathbf{a}(t) = \begin{bmatrix} a_1(t) \\ a_2(t) \\ \vdots \\ a_{N_s}(t) \end{bmatrix} \quad (5)$$

all of which are independent white Gaussian random processes with zero mean and unit PSD.

The transmitted signal at the transmitter array is

$$\mathbf{S}(t) = \mathbf{X}(t) * \mathbf{a}(t) \quad (6)$$

where $*$ represents convolution operator and each entry of $\mathbf{S}(t)$ is

$$S_i(t) = \sum_{j=1}^{N_s} (X_{ij}(t) * a_j(t)), \quad i = 1, 2, \dots, N_t \quad (7)$$

and the PSD of the transmitted signal at the transmitter array is

$$\mathbf{R}_S(f) = \mathbf{X}(f) \mathbf{X}^H(f) \quad (8)$$

where H represents conjugate transpose operator.

The received signal at the receiver array is

$$\mathbf{R}(t) = \mathbf{H}(t) * \mathbf{S}(t) + \mathbf{N}(t) \quad (9)$$

where $\mathbf{N}(t)$ is the additive white Gaussian noise the entries of which are independent random processes with zero mean and one-sided PSD N_0 .

If one-sided situation is considered, then the transmitted power is

$$P = \int_{f_0}^{f_1} \text{tr}[\mathbf{R}_S(f)] df \quad (10)$$

The equivalent ratio of the transmitted signal power to the received noise power (TX SNR) is defined as

$$\rho = \frac{P}{N_0 W} \quad (11)$$

The spectral efficiency is [8]

$$\frac{C}{W} = \frac{1}{W} \int_{f_0}^{f_1} \log_2 \left| \mathbf{I}_{N_r}(f) + \frac{\mathbf{H}(f) \mathbf{R}_S(f) \mathbf{H}^H(f)}{N_0} \right| df \quad (12)$$

Where $|\bullet|$ represents the determinant of the matrix.

A. Water Filling

It is well known that the spectral efficiency of water filling is greater than that of any other spectrum-shaping scheme. Let $\lambda_i(f)$, $i = 1, 2, \dots, N_t$ denote the set of eigenvalues of $N_0 \mathbf{H}^{-1}(f) [\mathbf{H}^{-1}(f)]^H$. So the singular value decomposition (SVD) of $N_0 \mathbf{H}^{-1}(f) [\mathbf{H}^{-1}(f)]^H$ can be written as

$$N_0 \mathbf{H}^{-1}(f) [\mathbf{H}^{-1}(f)]^H = \mathbf{U}(f) \text{diag} \{ \lambda_i(f) \} \mathbf{U}^H(f) \quad (13)$$

where $\text{diag}(\mathbf{a})$, if \mathbf{a} is a vector with n components, returns an n -by- n diagonal matrix having \mathbf{a} as its main diagonal. Because of the property of unitary matrix, $\frac{\mathbf{H}^H(f) \mathbf{H}(f)}{N_0}$ can be expressed as

$$\frac{\mathbf{H}^H(f) \mathbf{H}(f)}{N_0} = \mathbf{U}(f) \text{diag} \{ \lambda_i^{-1}(f) \} \mathbf{U}^H(f) \quad (14)$$

Then, $\mathbf{R}_S(f)$ can be given by

$$\mathbf{R}_S(f) = \mathbf{U}(f) \text{diag} \{ \Lambda_i(f) \} \mathbf{U}^H(f) \quad (15)$$

where $\Lambda_i(f) = (\mu - \lambda_i(f))^+$, $i = 1, 2, \dots, N_t$ and $(x)^+ = \max[0, x]$. Here, the constant μ is the water level chosen to satisfy the power constraint with equality

$$\sum_{i=1}^{N_t} \int_{f_0}^{f_1} \Lambda_i(f) df = P \quad (16)$$

So, the spectral efficiency $\frac{C}{W}$ in this case is [5]

$$\frac{1}{W} \sum_{i=1}^{N_t} \int_{f_0}^{f_1} \left(\log_2 \left(\frac{\mu}{\lambda_i(f)} \right) \right)^+ df \quad (17)$$

In order to decrease the computational complexity of spectral efficiency in water filling, the asymptotic behaviors of spectral efficiency for both very large and very small ρ are studied here according to [9]. For this purpose, let $\mu^\#$ be

$$\mu^\# = \frac{\mu}{N_0} \quad (18)$$

let $\lambda_i^\#(f)$ be

$$\lambda_i^\#(f) = \frac{\lambda_i(f)}{N_0}, \quad f_0 \leq f \leq f_1, \quad i = 1, 2, \dots, N_t \quad (19)$$

and the frequency band sets Ω_i , $i = 1, 2, \dots, N_t$ are defined for water level $\mu^\#$.

$$\Omega_i = \left\{ f : \lambda_i^\#(f) \leq \mu^\#; f_0 \leq f \leq f_1 \right\} \quad (20)$$

The measure of Ω_i is θ_i and

$$\theta = \frac{\sum_{i=1}^{N_t} \theta_i}{N_t} \quad (21)$$

Two average channel parameters are defined as [9].

$$\bar{\lambda} = \frac{\sum_{i=1}^{N_t} \int_{\Omega_i} \lambda_i^\#(f) df}{N_t \theta} \quad (22)$$

and

$$\bar{\lambda}_{\log} = \frac{\sum_{i=1}^{N_t} \int_{\Omega_i} \log_2 \left(\lambda_i^\#(f) \right) df}{N_t \theta} \quad (23)$$

From the power constraint, we can get

$$P = \sum_{i=1}^{N_t} \int_{f_0}^{f_1} \Lambda_i(f) df \quad (24)$$

$$= \sum_{i=1}^{N_t} \int_{f_0}^{f_1} (\mu - \lambda_i(f))^+ df \quad (25)$$

$$= N_0 \sum_{i=1}^{N_t} \int_{f_0}^{f_1} \left(\mu^\# - \lambda_i^\#(f) \right)^+ df \quad (26)$$

$$= N_0 \theta N_t (\mu^\# - \bar{\lambda}) \quad (27)$$

From the spectral efficiency formula, we can get

$$\frac{C}{W} = \frac{1}{W} \sum_{i=1}^{N_t} \int_{f_0}^{f_1} \left(\log_2 \left(\frac{\mu}{\lambda_i(f)} \right) \right)^+ df \quad (28)$$

$$= \frac{1}{W} \sum_{i=1}^{N_t} \int_{f_0}^{f_1} \left(\log_2 \left(\frac{\mu^\#}{\lambda_i^\#(f)} \right) \right)^+ df \quad (29)$$

$$= \frac{\theta N_t (\log_2 \mu^\# - \bar{\lambda}_{\log})}{W} \quad (30)$$

These equations are combined to yield

$$\frac{C}{W} = \frac{\theta N_t \left(\log_2 \left(\frac{P}{N_0 \theta N_t} + \bar{\lambda} \right) - \bar{\lambda}_{\log} \right)}{W} \quad (31)$$

$$= \frac{\theta N_t \left(\log_2 \left(\frac{P}{N_0 \theta N_t \lambda} + 1 \right) + \log_2 (\bar{\lambda}) - \bar{\lambda}_{\log} \right)}{W} \quad (32)$$

If P is large enough so that $\lambda_i^\#(f) \leq \mu^\#$ for all $f_0 \leq f \leq f_1$ and $i = 1, 2, \dots, N_t$, then $\theta = W$ as well as

$$\frac{C}{W} = \frac{W N_t \left(\log_2 \left(\frac{P}{N_0 W N_t \lambda} + 1 \right) + \log_2 (\bar{\lambda}) - \bar{\lambda}_{\log} \right)}{W} \quad (33)$$

$$= N_t \left(\log_2 \left(\frac{\rho}{N_t \lambda} + 1 \right) + \log_2 (\bar{\lambda}) - \bar{\lambda}_{\log} \right) \quad (34)$$

So, when $(\rho/N_t) \gg \bar{\lambda}$, then [9]

$$\frac{C}{W} \approx N_t \left(\log_2 \left(\frac{\rho}{N_t} \right) - \bar{\lambda}_{\log} \right) \quad (35)$$

This asymptotic behavior of spectral efficiency can be treated as the lower bound of the real spectral efficiency when P is sufficiently large.

If P is small enough, then

$$\frac{C}{W} = \frac{\theta N_t \left(\log_2 \left(\frac{P}{N_0 \theta N_t \lambda} + 1 \right) + \log_2 (\bar{\lambda}) - \bar{\lambda}_{\log} \right)}{W} \quad (36)$$

$$= \frac{\frac{\theta N_t}{\ln 2} \ln \left(\frac{P}{N_0 \theta N_t \lambda} + 1 \right) + \theta N_t (\log_2 (\bar{\lambda}) - \bar{\lambda}_{\log})}{W} \quad (37)$$

$$\leq \frac{\frac{P}{N_0 \lambda \ln 2} + \theta N_t (\log_2 (\bar{\lambda}) - \bar{\lambda}_{\log})}{W} \quad (38)$$

$$= \frac{\rho}{\bar{\lambda} \ln 2} + \frac{\rho (\log_2 (\bar{\lambda}) - \bar{\lambda}_{\log})}{\mu^\# - \bar{\lambda}} \quad (39)$$

When ρ approaches 0, $\mu^\#$ and $\bar{\lambda}$ approach λ_{\min} , where

$$\lambda_{\min} = \min \left\{ \lambda_i^\#(f) \mid f_0 \leq f \leq f_1, i = 1, 2, \dots, N_t \right\} \quad (40)$$

and [9]

$$\lim_{\rho \rightarrow 0} \frac{\log_2 (\bar{\lambda}) - \bar{\lambda}_{\log}}{\mu^\# - \bar{\lambda}} = 0 \quad (41)$$

Hence,

$$\frac{C}{W} \approx \frac{\rho}{\lambda_{\min} \ln 2} \quad (42)$$

This asymptotic behavior of spectral efficiency can be treated as the upper bound of the real spectral efficiency when P is sufficiently small.

B. Constant Power Water Filling

Constant power water filling is well studied in [7]. For water filling, the power allocation scheme is $\Lambda_i(f) = (\mu - \lambda_i(f))^+$, $i = 1, 2, \dots, N_t$. While for constant power water filling, the power allocation scheme is

$$\Lambda_i(f) = \begin{cases} p_0, & \text{if } \lambda_i(f) \leq \lambda_0 \\ 0, & \text{if } \lambda_i(f) > \lambda_0 \end{cases} \quad (43)$$

How to get the optimal p_0 and λ_0 is the key point of constant power water filling. Similarly, the frequency band sets $\Omega_i, i = 1, 2, \dots, N_t$ are defined as,

$$\Omega_i = \{f : \lambda_i(f) \leq \lambda_0; f_0 \leq f \leq f_1\} \quad (44)$$

The measure of Ω_i is θ_i and

$$\theta = \sum_{i=1}^{N_t} \theta_i \quad (45)$$

λ_0 should be chosen to meet the condition that $\min\{\lambda_i(f), f \in \Omega_i, i = 1, 2, \dots, N_t\} + \frac{P}{\theta}$ is equal to $\max\{\lambda_i(f), f \in \Omega_i, i = 1, 2, \dots, N_t\}$. Meanwhile, $p_0 = \frac{P}{\theta}$.

C. Time Reversal

For time reversal, it follows that

$$\mathbf{X}(f) = \alpha \mathbf{H}^H(f) \quad (46)$$

the constant α is the scale factor chosen to satisfy the power constraint with equality.

$$P = \int_{f_0}^{f_1} \text{tr}[\mathbf{R}_S(f)]df \quad (47)$$

$$= \int_{f_0}^{f_1} \text{tr}[\mathbf{X}(f) \mathbf{X}^H(f)]df \quad (48)$$

$$= \alpha^2 \int_{f_0}^{f_1} \text{tr}[\mathbf{H}^H(f) \mathbf{H}(f)]df \quad (49)$$

$$= \alpha^2 \int_{f_0}^{f_1} \sum_{i=1}^{N_r} \sum_{j=1}^{N_t} |H_{ij}(f)|^2 df \quad (50)$$

with,

$$\alpha = \sqrt{\frac{P}{\int_{f_0}^{f_1} \sum_{i=1}^{N_r} \sum_{j=1}^{N_t} |H_{ij}(f)|^2 df}} \quad (51)$$

so,

$$\mathbf{X}(f) = \sqrt{\frac{P}{\int_{f_0}^{f_1} \sum_{i=1}^{N_r} \sum_{j=1}^{N_t} |H_{ij}(f)|^2 df}} \mathbf{H}^H(f) \quad (52)$$

The spectral efficiency $\frac{C}{W}$ in this case is [5]

$$\frac{1}{W} \int_{f_0}^{f_1} \log_2 \left| \mathbf{I} + \frac{\rho W \mathbf{H}(f) \mathbf{H}^H(f) \mathbf{H}(f) \mathbf{H}^H(f)}{\int_{f_0}^{f_1} \sum_{i=1}^{N_r} \sum_{j=1}^{N_t} |H_{ij}(f)|^2 df} \right| df \quad (53)$$

D. Channel Inverse

For channel inverse, it follows that

$$\mathbf{X}(f) = \alpha \mathbf{H}^H(f) [\mathbf{H}(f) \mathbf{H}^H(f)]^{-1} \quad (54)$$

the constant α is the scale factor chosen to satisfy the power constraint with equality.

$$P = \int_{f_0}^{f_1} \text{tr}[\mathbf{R}_S(f)]df \quad (55)$$

$$= \int_{f_0}^{f_1} \text{tr}[\mathbf{X}(f) \mathbf{X}^H(f)]df \quad (56)$$

$$= \alpha^2 \int_{f_0}^{f_1} \text{tr}[[\mathbf{H}(f) \mathbf{H}^H(f)]^{-1}]df \quad (57)$$

with,

$$\alpha = \sqrt{\frac{P}{\int_{f_0}^{f_1} \text{tr}[[\mathbf{H}(f) \mathbf{H}^H(f)]^{-1}]df}} \quad (58)$$

so,

$$\mathbf{X}(f) = \sqrt{\frac{P}{\int_{f_0}^{f_1} \text{tr}[[\mathbf{H}(f) \mathbf{H}^H(f)]^{-1}]df}} \mathbf{H}^H(f) [\mathbf{H}(f) \mathbf{H}^H(f)]^{-1} \quad (59)$$

The spectral efficiency $\frac{C}{W}$ in this case is [5]

$$N_r \log_2 \left(1 + \frac{\rho W}{\int_{f_0}^{f_1} \text{tr}[[\mathbf{H}(f) \mathbf{H}^H(f)]^{-1}]df} \right) \quad (60)$$

E. Constant Power Spectrum Density

If power is equally allocated to each transmitter antenna, then

$$\mathbf{R}_S(f) = \frac{P}{WN_t} \mathbf{I}(f) \quad (61)$$

The spectral efficiency $\frac{C}{W}$ in this case is [5]

$$\frac{1}{W} \int_{f_0}^{f_1} \log_2 \left| \mathbf{I} + \frac{\rho \mathbf{H}(f) \mathbf{H}^H(f)}{N_t} \right| df \quad (62)$$

F. Minimum Mean Square Error

For MMSE, it follows that

$$\mathbf{X}(f) = \alpha \mathbf{H}^H(f) [\mathbf{H}(f) \mathbf{H}^H(f) + \frac{N_r}{\rho} \mathbf{I}]^{-1} \quad (63)$$

the constant α is the scale factor chosen to satisfy the power constraint with equality.

$$P = \int_{f_0}^{f_1} \text{tr}[\mathbf{R}_S(f)]df \quad (64)$$

$$= \int_{f_0}^{f_1} \text{tr}[\mathbf{X}(f) \mathbf{X}^H(f)]df \quad (65)$$

and

$$\mathbf{X}(f) \mathbf{X}^H(f) = \alpha^2 \int_{f_0}^{f_1} \text{tr} \left[\mathbf{H}^H(f) \left[\mathbf{H}(f) \mathbf{H}^H(f) + \frac{N_r}{\rho} \mathbf{I} \right]^{-2} \mathbf{H}(f) \right] df \quad (66)$$

So α is equal to

$$\sqrt{\frac{P}{\int_{f_0}^{f_1} \text{tr} \left[\mathbf{H}^H(f) \left[\mathbf{H}(f) \mathbf{H}^H(f) + \frac{N_r}{\rho} \mathbf{I} \right]^{-2} \mathbf{H}(f) \right] df}} \quad (67)$$

Similarly, the spectral efficiency in this case can be calculated by Equation 8 and Equation 12.

III. SPECTRAL EFFICIENCY OF TIME REVERSAL WITH POWER ALLOCATION

In this section, spectral efficiency of time reversal with power allocation is considered. How to allocate the power among the entries in the transmitted signal vector to maximize the spectral efficiency is studied. Two optimization problems are presented. The first problem is the extension of Equation 6. And in the second problem, there is only one independent entry in the transmitted signal vector.

A. Time Reversal with Multiplexing Gain

$\mathbf{H}(f)$, $\mathbf{H}(t)$, $\mathbf{X}(t)$, $\mathbf{X}(f)$ and $\mathbf{a}(t)$ are give in Equation 1, Equation 2, Equation 3, Equation 4 and Equation 5 respectively. Let us define the $N_s \times N_s$ diagonal power allocation matrix \mathbf{P} ,

$$\mathbf{P} = \begin{bmatrix} P_1 & & & \\ & P_2 & & \\ & & \ddots & \\ & & & P_{N_s} \end{bmatrix} \quad (68)$$

Thus, the transmitted signal at the transmitter array is

$$\mathbf{S}(t) = \mathbf{X}(t) * \left(\sqrt{\mathbf{P}} \mathbf{a}(t) \right) \quad (69)$$

and the PSD of the transmitted signal at the transmitter array is

$$\mathbf{R}_S(f) = \mathbf{X}(f) \mathbf{P} \mathbf{X}^H(f) \quad (70)$$

For time reversal scheme, it follows that

$$\mathbf{X}(f) = \mathbf{H}^H(f) \quad (71)$$

and $N_s = N_r$.

If one-sided situation is considered, then the total transmitted power is

$$P_t = \int_{f_0}^{f_1} \text{tr} [\mathbf{R}_S(f)] df \quad (72)$$

$$= \int_{f_0}^{f_1} \text{tr} [\mathbf{X}(f) \mathbf{P} \mathbf{X}^H(f)] df \quad (73)$$

$$= \int_{f_0}^{f_1} \text{tr} [\mathbf{H}^H(f) \mathbf{P} \mathbf{H}(f)] df \quad (74)$$

$$= \int_{f_0}^{f_1} \text{tr} [\mathbf{P} \mathbf{H}(f) \mathbf{H}^H(f)] df \quad (75)$$

The spectral efficiency $\frac{C}{W}$ in this case is [10]

$$\frac{1}{W} \int_{f_0}^{f_1} \log_2 \left| \mathbf{I} + \frac{\mathbf{P} \mathbf{H}(f) \mathbf{H}^H(f) \mathbf{H}(f) \mathbf{H}^H(f)}{N_0} \right| df \quad (76)$$

How to get the optimal P_i , $i = 1, 2, \dots, N_r$ to achieve the optimal spectral efficiency is studied here. So the corresponding optimization problem can be described as

$$\begin{aligned} & \max \frac{1}{W} \int_{f_0}^{f_1} \log_2 \left| \mathbf{I} + \frac{\mathbf{P} \mathbf{H}(f) \mathbf{H}^H(f) \mathbf{H}(f) \mathbf{H}^H(f)}{N_0} \right| df \\ & \text{s.t.} \quad \int_{f_0}^{f_1} \text{tr} [\mathbf{P} \mathbf{H}(f) \mathbf{H}^H(f)] df \leq P \\ & \mathbf{P} = \begin{bmatrix} P_1 & & & \\ & P_2 & & \\ & & \ddots & \\ & & & P_{N_r} \end{bmatrix} \\ & P = \rho N_0 (f_1 - f_0) \\ & P_i \geq 0, \quad i = 1, 2, \dots, N_r \end{aligned} \quad (77)$$

where ρ is defined in Equation 11.

If $\beta_i = \int_{f_0}^{f_1} [\mathbf{H}(f) \mathbf{H}^H(f)]_{i,i} df$, $i = 1, 2, \dots, N_r$ and equality constraint is considered, then $\sum_{i=1}^{N_r} \beta_i P_i = P$. If $\beta = [\beta_1 \beta_2 \dots \beta_{N_r}]$ and $\mathbf{p} = [P_1 P_2 \dots P_{N_r}]^T$, where T represents the transpose operator, then the equality constraint can be further simplified as,

$$\beta \mathbf{p} = P \quad (78)$$

Define,

$$\Psi(f) = \mathbf{H}(f) \mathbf{H}^H(f) \mathbf{H}(f) \mathbf{H}^H(f) / N_0 \quad (79)$$

$$\Xi(f) = \mathbf{I} + \mathbf{P} \Psi(f) \quad (80)$$

$$C_f(\mathbf{p}) = \log_2 |\Xi(f)| \quad (81)$$

and

$$C(\mathbf{p}) = \int_{f_0}^{f_1} C_f(\mathbf{p}) df \quad (82)$$

According to the concavity of $\log_2 |\bullet|$ and the affine transformation, $C_f(\mathbf{p})$ is concave in P_i , $i = 1, 2, \dots, N_r$ [11] [12]. Further more, $C(\mathbf{p})$ is also concave in P_i , $i = 1, 2, \dots, N_r$.

According to the barrier method [11], $C_0(\mathbf{p})$ and $\phi(\mathbf{p})$ are defined as,

$$C_0(\mathbf{p}) = -C(\mathbf{p}) \quad (83)$$

and

$$\phi(\mathbf{p}) = - \sum_{i=1}^{N_r} \log(P_i (P - \beta_i P_i)) \quad (84)$$

Given strictly feasible \mathbf{p} , for example, P_i , $i = 1, 2, \dots, N_r$ are set equally. $t > 0$, $\mu > 1$ and $\varepsilon > 0$. The optimal \mathbf{p} can be obtained by the following iterative numerical method.

Repeat:

1 Compute $\mathbf{p}(t)$ by minimizing $f = tC_0 + \phi$, subject to $\beta \mathbf{p} = P$.

2 $\mathbf{p} := \mathbf{p}(t)$.

3 If $N_r/t < \varepsilon$, stop, else $t := \mu t$.

The newton method [11] can be used to solve the minimizing problem in the first step. $\Delta \mathbf{p}$ is defined as the newton step at \mathbf{p} and $\Delta \mathbf{p}$ can be characterized by

$$\begin{bmatrix} \nabla^2 f(\mathbf{p}) & \beta^T \\ \beta & 0 \end{bmatrix} \begin{bmatrix} \Delta \mathbf{p} \\ w \end{bmatrix} = \begin{bmatrix} -\nabla f(\mathbf{p}) \\ 0 \end{bmatrix} \quad (85)$$

where

$$\nabla f(\mathbf{p}) = \left[\frac{\partial f(\mathbf{p})}{\partial P_1} \quad \frac{\partial f(\mathbf{p})}{\partial P_2} \quad \dots \quad \frac{\partial f(\mathbf{p})}{\partial P_{N_r}} \right]^T \quad (86)$$

and

$$\nabla^2 f(\mathbf{p}) = \begin{bmatrix} \frac{\partial^2 f(\mathbf{p})}{\partial P_1 \partial P_1} & \frac{\partial^2 f(\mathbf{p})}{\partial P_1 \partial P_2} & \dots & \frac{\partial^2 f(\mathbf{p})}{\partial P_1 \partial P_{N_r}} \\ \frac{\partial^2 f(\mathbf{p})}{\partial P_2 \partial P_1} & \frac{\partial^2 f(\mathbf{p})}{\partial P_2 \partial P_2} & \dots & \frac{\partial^2 f(\mathbf{p})}{\partial P_2 \partial P_{N_r}} \\ \vdots & \vdots & \ddots & \vdots \\ \frac{\partial^2 f(\mathbf{p})}{\partial P_{N_r} \partial P_1} & \frac{\partial^2 f(\mathbf{p})}{\partial P_{N_r} \partial P_2} & \dots & \frac{\partial^2 f(\mathbf{p})}{\partial P_{N_r} \partial P_{N_r}} \end{bmatrix} \quad (87)$$

$\partial f(\mathbf{p})/\partial P_i$, $i = 1, 2, \dots, N_r$ is derived as,

$$\begin{aligned} & \frac{\partial f(\mathbf{p})}{\partial P_i} \\ &= -t \int_{f_0}^{f_1} \frac{\sum_{m=1}^{N_r} (-1)^{i+m} [\Psi(f)]_{i,m} \left| [\Xi(f)]_{i,m,\text{sub}} \right|}{\left| \Xi(f) \right| \log 2} df \\ & - \frac{P - 2\beta_i P_i}{P_i (P - \beta_i P_i)} \end{aligned} \quad (88)$$

where $[\Xi(f)]_{i,m,\text{sub}}$ is the sub-matrix which is obtained from $\Xi(f)$ when the entries in the i th row and the m th column are removed.

If $i = j$, $i = 1, 2, \dots, N_r$, $j = 1, 2, \dots, N_r$, then $\frac{\partial^2 f(\mathbf{p})}{\partial P_i \partial P_j}$ is derived as,

$$\begin{aligned} & \frac{\partial^2 f(\mathbf{p})}{\partial P_i \partial P_j} \\ &= t \int_{f_0}^{f_1} \frac{\left(\sum_{m=1}^{N_r} (-1)^{i+m} [\Psi(f)]_{i,m} \left| [\Xi(f)]_{i,m,\text{sub}} \right| \right)^2}{\left| \Xi(f) \right|^2 \log 2} df \\ & - g_1 \end{aligned} \quad (89)$$

where

$$g_1 = \frac{2\beta_i P_i P - 2\beta_i^2 P_i^2 - P^2}{P_i^2 (P - \beta_i P_i)^2} \quad (90)$$

If $i \neq j$, $i = 1, 2, \dots, N_r$, $j = 1, 2, \dots, N_r$, then $\frac{\partial^2 f(\mathbf{p})}{\partial P_i \partial P_j}$ is derived as,

$$\frac{\partial^2 f(\mathbf{p})}{\partial P_i \partial P_j} = -t \int_{f_0}^{f_1} \frac{T(f)}{\left| \Xi(f) \right|^2 \log 2} df \quad (91)$$

where

$$\begin{aligned} T(f) &= \left| \Xi(f) \right| \sum_{m=1}^{N_r} \left((-1)^{i+m} [\Psi(f)]_{i,m} \frac{\partial \left(\left| [\Xi(f)]_{i,m,\text{sub}} \right| \right)}{\partial P_j} \right) \\ & - \frac{\partial \left(\left| \Xi(f) \right| \right)}{\partial P_j} \sum_{m=1}^{N_r} (-1)^{i+m} [\Psi(f)]_{i,m} \left| [\Xi(f)]_{i,m,\text{sub}} \right| \end{aligned} \quad (92)$$

If $j > i$, then $\partial \left(\left| [\Xi(f)]_{i,m,\text{sub}} \right| \right) / \partial P_j$ is equal to

$$\begin{aligned} & \sum_{n=1}^{m-1} (-1)^{j-1+n} [\Psi(f)]_{j,n} \left| \left([\Xi(f)]_{i,m,\text{sub}} \right)_{j-1,n,\text{sub}} \right| \\ & + \sum_{n=m+1}^{N_r} (-1)^{j-1+n-1} [\Psi(f)]_{j,n} \left| \left([\Xi(f)]_{i,m,\text{sub}} \right)_{j-1,n-1,\text{sub}} \right| \end{aligned} \quad (93)$$

If $j < i$, then $\partial \left(\left| [\Xi(f)]_{i,m,\text{sub}} \right| \right) / \partial P_j$ is equal to

$$\begin{aligned} & \sum_{n=1}^{m-1} (-1)^{j+n} [\Psi(f)]_{j,n} \left| \left([\Xi(f)]_{i,m,\text{sub}} \right)_{j,n,\text{sub}} \right| \\ & + \sum_{n=m+1}^{N_r} (-1)^{j+n-1} [\Psi(f)]_{j,n} \left| \left([\Xi(f)]_{i,m,\text{sub}} \right)_{j,n-1,\text{sub}} \right| \end{aligned} \quad (94)$$

$\partial \left(\left| \Xi(f) \right| \right) / \partial P_j$ is equal to

$$\sum_{m=1}^{N_r} (-1)^{j+m} [\Psi(f)]_{j,m} \left| [\Xi(f)]_{j,m,\text{sub}} \right| \quad (95)$$

B. Time Reversal with Array Gain

If $\mathbf{a}(t)$ is expressed as

$$\mathbf{a}(t) = \mathbf{L} a(t) \quad (96)$$

where $a(t)$ is the white Gaussian random process with zero mean and unit PSD. \mathbf{L} can be similarly treated as the power allocation vector,

$$\mathbf{L} = \begin{bmatrix} L_1 \\ L_2 \\ \vdots \\ L_{N_s} \end{bmatrix} \quad (97)$$

In this situation, there is only one independent entry in $\mathbf{a}(t)$, which is called time reversal with array gain in this paper.

Thus, the transmitted signal at the transmitter array is

$$\mathbf{S}(t) = \mathbf{X}(t) * \mathbf{a}(t) \quad (98)$$

$$= \mathbf{X}(t) * (\mathbf{L} a(t)) \quad (99)$$

and the PSD of the transmitted signals at the transmitter array is

$$\mathbf{R}_S(f) = \mathbf{X}(f) \mathbf{L} \mathbf{L}^T \mathbf{X}^H(f) \quad (100)$$

For time reversal scheme, it follows that

$$\mathbf{X}(f) = \mathbf{H}^H(f) \quad (101)$$

and $N_s = N_r$.

If one-sided situation is considered, then the total transmitted power is

$$P_t = \int_{f_0}^{f_1} \text{tr} [\mathbf{R}_S(f)] df \quad (102)$$

$$= \int_{f_0}^{f_1} \text{tr} [\mathbf{X}(f) \mathbf{L} \mathbf{L}^T \mathbf{X}^H(f)] df \quad (103)$$

$$= \int_{f_0}^{f_1} \text{tr} [\mathbf{H}^H(f) \mathbf{L} \mathbf{L}^T \mathbf{H}(f)] df \quad (104)$$

$$= \int_{f_0}^{f_1} \text{tr} [\mathbf{L} \mathbf{L}^T \mathbf{H}(f) \mathbf{H}^H(f)] df \quad (105)$$

The spectral efficiency $\frac{C}{W}$ in this case is [10]

$$\frac{1}{W} \int_{f_0}^{f_1} \log_2 \left| \mathbf{I} + \frac{\mathbf{L}\mathbf{L}^T \mathbf{H}(f) \mathbf{H}^H(f) \mathbf{H}(f) \mathbf{H}^H(f)}{N_0} \right| df \quad (106)$$

Similarly, how to get the optimal L_i , $i = 1, 2, \dots, N_r$ to achieve the optimal spectral efficiency is studied here. So the corresponding optimization problem can be described as

$$\begin{aligned} \max \quad & \frac{1}{W} \int_{f_0}^{f_1} \log_2 \left| \mathbf{I} + \frac{\mathbf{L}\mathbf{L}^T \mathbf{H}(f) \mathbf{H}^H(f) \mathbf{H}(f) \mathbf{H}^H(f)}{N_0} \right| df \\ \text{s.t.} \quad & \int_{f_0}^{f_1} \text{tr} [\mathbf{L}\mathbf{L}^T \mathbf{H}(f) \mathbf{H}^H(f)] df \leq P \\ & \mathbf{L} = \begin{bmatrix} L_1 \\ L_2 \\ \vdots \\ L_{N_r} \end{bmatrix} \\ & P = \rho N_0 (f_1 - f_0) \\ & L_i \geq 0, i = 1, 2, \dots, N_r \end{aligned} \quad (107)$$

where ρ is defined in Equation 11.

Define,

$$\Psi(f) = \mathbf{H}(f) \mathbf{H}^H(f) \mathbf{H}(f) \mathbf{H}^H(f) / N_0 \quad (108)$$

$$\Upsilon(f) = \mathbf{H}(f) \mathbf{H}^H(f) \quad (109)$$

$$\begin{aligned} C(\mathbf{L}) &= \int_{f_0}^{f_1} \log_2 \left| \mathbf{I}(f) + \mathbf{L}\mathbf{L}^T \Psi(f) \right| df \quad (110) \\ &= \int_{f_0}^{f_1} \log_2 (1 + \mathbf{L}^T \Psi(f) \mathbf{L}) df \quad (111) \end{aligned}$$

and

$$h(\mathbf{L}) = \int_{f_0}^{f_1} (\mathbf{L}^T \Upsilon(f) \mathbf{L}) df - P \quad (112)$$

Even though the first and second derivatives of the objective function and constraint function can be easily derived [10], because the objective function is a nonlinear and nonconvex function, it is hard to use deterministic algorithm to solve the optimization problem 107. In recent years, the random algorithm is widely used to solve the nonlinear and nonconvex optimization problem to get the near optimal solution. Here particle swarm optimization (PSO) is employed to solve the optimization problem 107.

PSO is a swarm intelligence based algorithm to find a solution to an optimization problem in a search space [13]. There are many particles with a position and a velocity in the swarm. Particles in a swarm communicate good positions to each other and adjust their own position and velocity based on these good positions [13]. There are two kinds of good positions: (1) a global best position that is known to all and immediately updated when a new best position is found by any particle in the swarm; (2) the local best position, which is the best solution that the particle has passed [13].

Suppose there are N particles in N_r -dimensional space. After K iterations, the algorithm is stopped. When the k th iteration begins, the position of particle i is \mathbf{L}_i^{k-1} . The

velocity of particle i is \mathbf{V}_i^{k-1} . The local best position of particle i is

$$\mathbf{L}_{i\text{best}}^k = \max_{\{\mathbf{L}_{i\text{best}}^{k-1}, \mathbf{L}_i^{k-1}\}} C(\mathbf{L}) \quad (113)$$

and the global best position is

$$\mathbf{L}_{\text{gbest}}^k = \max_{\{\mathbf{L}_{i\text{best}}^k, i=1,2,\dots,N\}} C(\mathbf{L}) \quad (114)$$

Then the velocity of particle i in the k th iteration is

$$\begin{aligned} \mathbf{V}_i^k &= w \times \mathbf{V}_i^{k-1} \\ &+ c_1 \times \text{rand} \times (\mathbf{L}_{i\text{best}}^k - \mathbf{L}_i^{k-1}) \\ &+ c_2 \times \text{rand} \times (\mathbf{L}_{\text{gbest}}^k - \mathbf{L}_i^{k-1}) \end{aligned} \quad (115)$$

and the new position of particle i is $\mathbf{L}_i^k = \mathbf{L}_i^{k-1} + \mathbf{V}_i^k$. In Equation 115, rand means random value drawn from a uniform distribution on the unit interval; w is the inertia weight; c_1 and c_2 are two positive constants, called the cognitive and social parameter respectively.

Meanwhile, if $h(\mathbf{L}_i^k) > 0$, which means the particle i moves to the infeasible position, then $C(\mathbf{L}_i^k)$ is set extremely small value. Although PSO can not guarantee the optimal solution, it can still find the solution very close to the optimal solution.

IV. CHANNEL SOUNDING

Channel sounding is performed using frequency domain technique to get MIMO UWB channel transfer function $\mathbf{H}(f)$ in confined metal environment. In channel sounding, rectangular metal cavity, the size of which is 8 feet by 8 feet by 8 feet, is used to emulate confined metal environment [14]. The material of cavity is aluminum.

The data of channel transfer function is collected using VNA - Agilent N5230A (300 kHz -13.5 GHz). It sweeps from 3 GHz to 10 GHz using 7001 tones with frequency step of 1 MHz. The power of each tone is 10 dBm. The averaging number is 128, which enhances the accuracy of channel sounding. Meanwhile, the cables and the connectors are calibrated before channel sounding to compensate for the frequency dependent losses.

The setup of channel sounding is shown in Figure 2 and the basic parameters for channel sounding are given by Table I. There are three antennas in the transmitter array and three antennas in the receiver array. Virtual array technique is employed here. The distance between the transmitter array and the receiver array is 4 feet. The distance between the antennas in the array is 2 feet. The antenna is placed at 1.35 meters above the ground. The channel transfer function from transmitter antenna two to receiver antenna two is shown in Figure 3 as an example.

V. NUMERICAL RESULTS

In this section, we give the numerical results of spectral efficiency for MIMO UWB channel in rectangular metal cavity. Figure 4 and Figure 5 show spectral efficiencies in rectangular metal cavity when different spectrum-shaping schemes are employed. Figure 4 uses the log expression

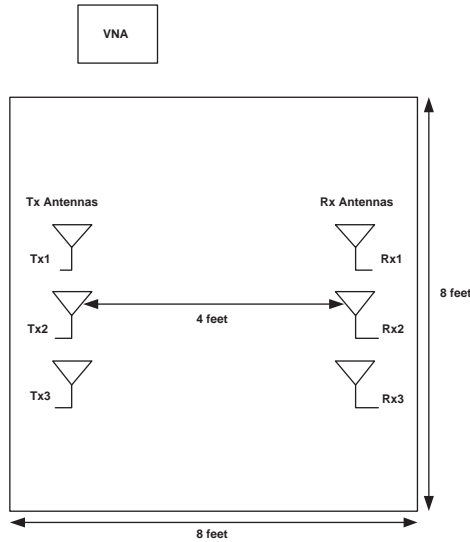


Figure 2. The setup of channel sounding.

TABLE I.
CHANNEL SOUNDING PARAMETERS

Parameter	Value
Frequency Band	3GHz-10GHz
Bandwidth	7GHz
Number of Points	7001
Transmitted Power	10dBm
Frequency Step	1MHz
Antenna Polarization	vertical
Averaging Number	128
Antenna Height	1.35 m

in the y axis to show the low TX SNR region clearly and Fig. 5 uses the linear expression in the y axis to show the high TX SNR region clearly. Figure 6 shows the spectral efficiency ratio of different spectrum-shaping schemes to water filling.

Water filling gives the maximum spectral efficiency among these schemes. Channel inverse is good for detection but performs poorly in terms of spectral efficiency. Time reversal does the tradeoff between detection and spectral efficiency. The spectrum efficiency of constant PSD is smaller than that of time reversal at low TX SNR and larger than that of time reversal at high TX SNR. Meanwhile spectral efficiency of constant PSD approaches that of water filling very well at high TX SNR. The constant PSD can be easily implemented, because channel state information is not needed at the transmitter. In real system, chirp signal generated by SAW device can be used to implement constant PSD. The spectral efficiency of constant power water filling is very close to that of water filling, but the computational complexity of the former is much lower than that of the latter. The spectral efficiency of MMSE is between the spectral efficiencies of time reversal and channel inverse. At low TX SNR, $[\mathbf{X}(f)]_{\text{MMSE}} \approx \frac{\rho\alpha}{N_r} \mathbf{H}^H(f)$, so the spectrum efficiency of MMSE is similar to that of time reversal. While at high TX SNR, $[\mathbf{X}(f)]_{\text{MMSE}} \approx \alpha \mathbf{H}^H(f) [\mathbf{H}(f) \mathbf{H}^H(f)]^{-1}$, so the spectral efficiency of MMSE is close to that of channel inverse.

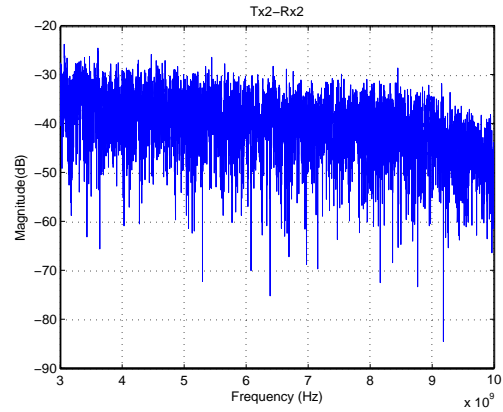


Figure 3. Channel Transfer Function.

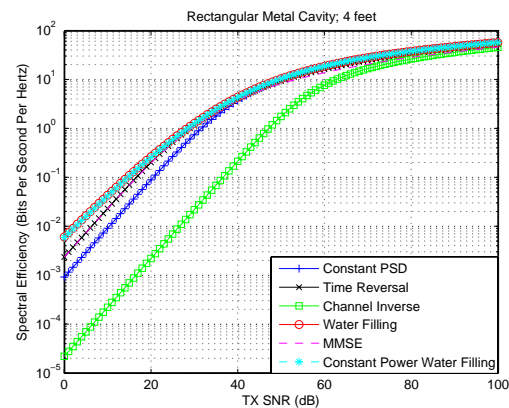


Figure 4. Spectral efficiency in rectangular metal cavity (Low TX SNR).

Figure 7 shows spectral efficiency of water filling if different antenna configurations are employed. At high TX SNR, the spectral efficiency of 3-by-3 is almost 4.7 dB larger than that of 1-by-1 and the spectral efficiency of 2-by-2 is almost 3 dB larger than that of 1-by-1. MIMO introduces apparent increase in spectral efficiency. Because maximum achievable data rate of the channel is unique if the system bandwidth, antenna configuration and total transmitted power are given, spectral efficiency of water filling can be used as the metric to quantify the channel.

Figure 8 shows spectral efficiency and its corresponding lower bound of water filling. This lower bound approaches the spectral efficiency at high TX SNR. If $\lambda_i^\#(f) \leq \mu^\#$ is not satisfied for all $f_0 \leq f \leq f_1$ and $i = 1, 2, \dots, N_t$, this bound is not valid. Figure 9 shows spectral efficiency and its corresponding upper bound of water filling. This bound is valid at low TX SNR. The advantage of this bound is that the bound is linear with TX SNR that can be used to estimate the spectral efficiency of water filling easily and quickly.

For the spectral efficiency of time reversal with power allocation, deterministic algorithm, i.e. the barrier method together with the newton method and random algorithm, i.e. PSO are used in this paper. In the barrier method, t is initially set 1; μ is set 2; ε is set 0.00000001. In PSO, the number of particles in the swarm is 200; the number

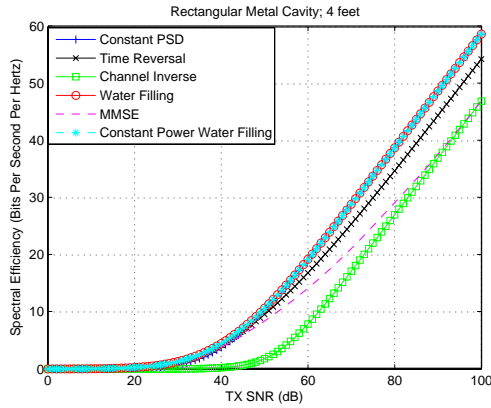


Figure 5. Spectral efficiency in rectangular metal cavity (High TX SNR).

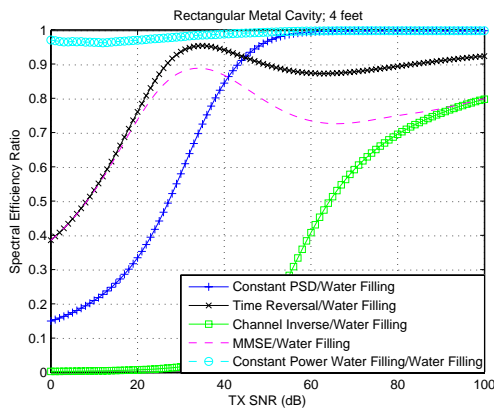


Figure 6. Spectral efficiency ratio in rectangular metal cavity.

of iterations is 150; w is set $\frac{\text{rand}}{2} + 0.5$; $c_1 = c_2 = 2$.

Figure 10 shows the spectral efficiency of time reversal with power allocation. Figure 11 shows the ratio of spectral efficiency of time reversal with array gain to that of time reversal with multiplexing gain. At high TX SNR, the spectral efficiency of time reversal with multiplexing gain is obviously larger than that of time reversal with array gain. While at low TX SNR, the spectral efficiency of time reversal with multiplexing gain is almost the same as that of time reversal with array gain. Multiplexing gain will be obvious at high TX SNR. While at low TX SNR, all the power should be allocated into one equivalent spatio-frequency channel which has the largest gain.

Figure 12 shows the ratio of spectral efficiency of time reversal without power allocation to that of time reversal with power allocation when multiplexing gain is considered. At high TX SNR, the spectral efficiency of time reversal without power allocation is almost the same as that of time reversal with power allocation, which means in this kind of SNR region, power allocation is not a must and equally allocating the power to each entry in the transmitted signal vector can reach the optimal spectral efficiency. At low TX SNR, there is a small gap between spectral efficiencies of time reversal without power allocation and with power allocation. From the solution of the optimization problem 77, the small power

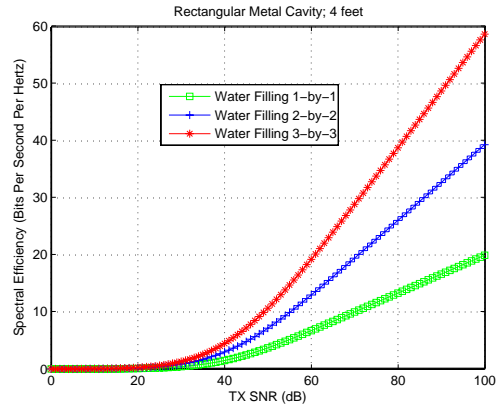


Figure 7. Spectral efficiency of water filling.

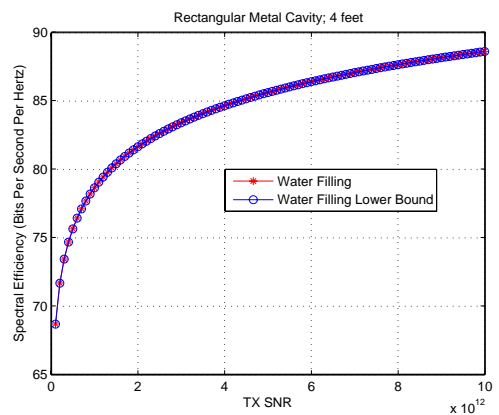


Figure 8. Spectral efficiency and its corresponding lower bound of water filling.

should be allocated to one entry which corresponds to the equivalent channel with the largest gain. Because the size of MIMO is small, i.e. 3-by-3 in this paper, power allocation can not bring the obvious improvement in spectral efficiency. This results tell us in the complex system, if the degree of freedom for power allocation is limited, constant power allocation can reach the near optimal performance.

VI. CONCLUSION

This paper considers spectral efficiency for MIMO UWB channel in rectangular metal cavity and calculates spectral efficiencies when different spectrum-shaping schemes are used. These spectrum-shaping schemes include water filling, time reversal, channel inverse, constant power spectrum density as well as constant power water filling, minimum mean square error. Meanwhile, spectral efficiency of time reversal with power allocation is considered. Deterministic algorithm and random algorithm are used to solve the corresponding optimization problems respectively in order to get the optimal spectral efficiency in time reversal.

ACKNOWLEDGMENT

This work is funded by the Office of Naval Research through a grant (N00014-07-1-0529), National Science

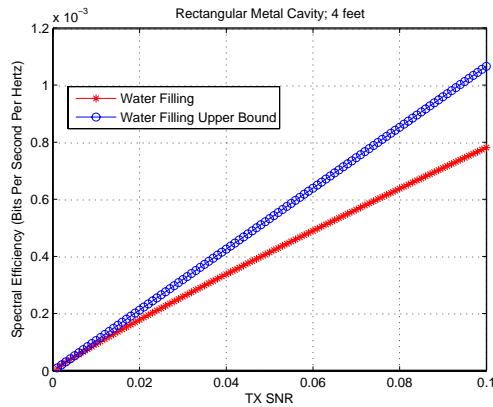


Figure 9. Spectral efficiency and its corresponding upper bound of water filling.

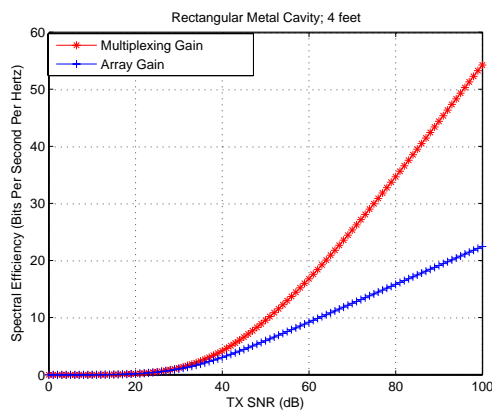


Figure 10. Spectral efficiency of time reversal with power allocation.

Foundation through a grant (ECS-0622125), the Army Research Laboratory and the Army Research Office through a STIR grant (W911NF-06-1-0349), a DURIP grant (W911NF-05-1-0111), and ONR Summer Faculty Fellowship Program Award.

The authors want to thank their sponsors Santanu K. Das (ONR), Brian Sadler (ARL), and Robert Ulman (ARO) for helpful discussions. The director of Center for Manufacturing Research (CMR) at TTU (Kenneth Currie) and the chair of ECE (Stephen Parke) at TTU have provided the authors with good support for carrying out this research. The authors also want to thank Nan Guo for assistance in channel sounding and helpful discussions. Finally, the authors would like to thank Bo Li in University of Florida for assistance in optimization problem.

REFERENCES

[1] R. C. Qiu, B. M. Sadler, and Z. Hu, "Time Reversed Transmission with Chirp Signaling for UWB Communications and Its Application in Confined Metal Environments," in *International Conference on Ultra-wideband, ICUWB'07*, (Singapore), September 2007.
 [2] R. C. Qiu, C. Zhou, J. Q. Zhang, and N. Guo, "Channel Reciprocity and Time-Reversed Propagation for Ultra-Wideband Communications," in *IEEE AP-S International Symposium on Antennas and Propagation, Honolulu, Hawaii*, vol. 1, June 2007.

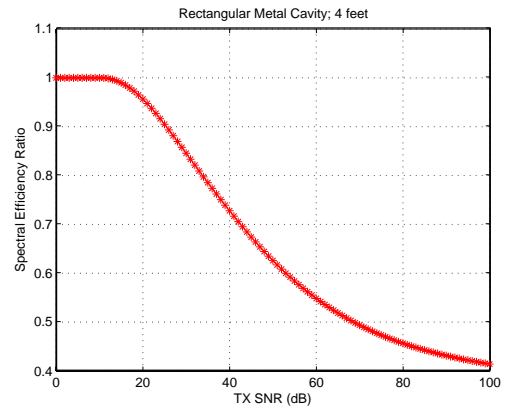


Figure 11. The ratio of spectral efficiency of time reversal with array gain to that of time reversal with multiplexing gain.

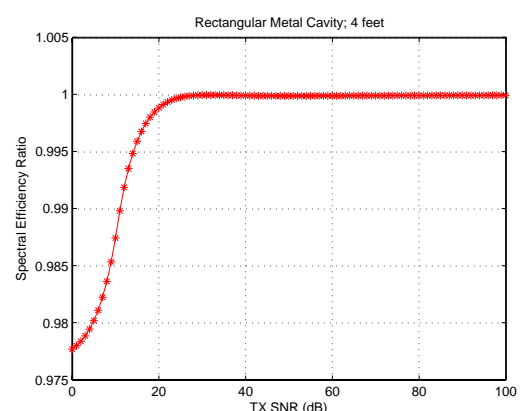


Figure 12. The ratio of spectral efficiency of time reversal without power allocation to that of time reversal with power allocation when multiplexing gain is considered.

[3] D. Singh, Z. Hu and R. Qiu, "UWB Channel Sounding and Channel Characteristics in Rectangular Metal Cavity," in *IEEE Southeastcon, 2008.*, Huntsville AL, 2008.
 [4] R. C. Qiu, "A Theory of Time-Reversed Impulse Multiple-Input Multiple-Output (MIMO) for Ultra-Wideband (UWB) Communications (invited paper)," in *2006 Int'l Conf. UWB*, October 2006.
 [5] Z. Hu, D. Singh and R. Qiu, "MIMO Capacity for UWB Channel in Rectangular Metal Cavity," in *IEEE Southeastcon, 2008.*, Huntsville AL, 2008.
 [6] Rachid Saadane, Aawatif Menouni, Raymond Knopp and Driss Aboutajdine, "Empirical Eigenanalysis of Indoor UWB Propagation Channels" in *IEEE Global Telecommunications Conference, 2004.*, VOL. 5, pp. 3215–3219, 2004.
 [7] Wei Yu and John M. Cioffi, "Constant-Power Waterfilling: Performance Bound and Low-Complexity Implementation," *IEEE TRANSACTIONS ON COMMUNICATIONS*, VOL. 54, NO. 1, pp. 23–28, January 2006.
 [8] A. Paulraj, R. Nabar and D. Gore, "Introduction to Space-Time Wireless Communications," Cambridge University Press, Cambridge England, 2003.
 [9] L. H. Brandenburg and A. D. Wyner, "Capacity of the Gaussian Channel with Memory: The Multivariate Case," *The Bell System Technical Journal*, Vol. 53, No. 5, pp. 745–778, May-June 1974.
 [10] Robert C. Qiu, "Time-Reversal Based Range Extension Technique for Ultra-wideband (UWB) Sensors and Applications in Tactical Communications and Networking,"

Technical Report (Quarterly) to US Office of Naval Research, July 2008.

- [11] Stephen Boyd and Lieven Vandenberghe, "Convex Optimization," Cambridge University Press, 2004.
- [12] Aditya Dua, Kamesh Medepalli, and Arogyaswami J. Paulraj, "Receive Antenna Selection in MIMO Systems using Convex Optimization," *IEEE TRANSACTIONS ON WIRELESS COMMUNICATIONS*, VOL. 5, NO. 9, pp. 2353–2357, September 2006
- [13] http://en.wikipedia.org/wiki/Particle_swarm_optimization.
- [14] <http://iweb.tntech.edu/rqiu/infrastructure.htm#labphotos>.

Zhen Hu (IEEE S'08) was born in Wuhan, China. He received the bachelor degree in Department of Electronics and Information Engineering from Huazhong University of Science and Technology, Wuhan, in 2004 and the master degree in National Mobile Communications Research Laboratory from Southeast University, Nanjing, in 2007. Now he pursues his Ph.D. in Tennessee Technological University, Cookeville. His research area is UWB system and optimization issues in wireless communication.

Robert Caiming Qiu (IEEE S'93-M'96-SM'01) received the Ph.D. degree in electrical engineering from New York University (former Polytechnic University, Brooklyn, NY). He is currently Professor in the Department of Electrical and Computer Engineering, Center for Manufacturing Research, Tennessee Technological University, Cookeville. His current interest is in wireless communication and networking systems, in particular Ultrawideband (UWB). He was Founder-CEO and President of Wiscom Technologies, Inc., manufacturing and marketing WCDMA chipsets. Wiscom was sold to Intel in 2003. Prior to Wiscom, he worked for GTE Labs, Inc. (now Verizon), Waltham, MA, and Bell Labs, Lucent, Whippany, NJ. He has worked in wireless communications, radio propagation, digital signal processing, EM scattering, composite absorbing materials, RF microelectronics, UWB, underwater acoustics, and fiber optics. He holds over 5 patents in WCDMA and authored over 50 journal papers/book chapters. He contributed to 3GPP and IEEE standards bodies, and delivered invited seminars to institutions including Princeton University and the U.S. Army Research Lab.

He served as an adjunct professor in Polytechnic University, Brooklyn, New York. Dr. Qiu serves as Associate Editor, *IEEE TRANSACTIONSONVEHICULAR TECHNOLOGY*, *International Journal of Sensor Networks (Inderscience)* and *Wireless Communication and Mobile Computing (NewYork: Wiley)*. He is a Guest Book Editor for *Ultra-Wideband (UWB)Wireless Communications (NewYork: Wiley, 2005)*, and three special issues on UWB including the *IEEE JOURNAL ON SELECTED AREAS IN COMMUNICATIONS*, *IEEE TRANSACTIONS ON VEHICULAR TECHNOLOGY*. He serves as a Member of TPC for GLOBE-COM, WCNC, and MILCOM. In addition, he served on the advisory board of the New Jersey Center for Wireless Telecommunications (NJCWT).

Dalwinder Singh was born in Punjab, India. He received the B.Tech degree in electronics and communication engineering with distinction from Punjab Technical University, Punjab, in 2006 and the M.S. degree in electrical engineering from Tennessee Technological University, Cookeville, in 2008. His research area was the capacity and sensing in UWB system.